Effect of Dissolved CO_2 in De-ionized Water in Reducing Wafer Damage During Megasonic Cleaning in MegPie®

S. Kumari [a], M. Keswani [a], S. Singh [b], M. Beck [c], E. Liebscher [c], L. Q. Toan [d] and S. Raghavan [a]

[a] Department of Materials Science and Engineering, The University of Arizona, Tucson, Arizona 85721, USA
[b] Department of Chemistry and Biochemistry, The University of Arizona, Tucson, Arizona 85721, USA
[c] Product Systems Incorporation, Campbell, California 95008, USA
[d] IMEC, Kapeldreef 75, 3001 Leuven, Belgium

Particle removal from wafer surfaces can be accomplished by irradiation of cleaning fluid by sound waves in the MHz frequency range. Unfortunately, unless proper cleaning conditions are chosen, megasonic irradiation may also result in damage to fragile wafer features. Here, we demonstrate a strong effect of dissolved CO_2 levels on the reduction of wafer damage during megasonic cleaning. Test structures with L/S patterns were irradiated with 0.93 MHz sound waves at varying power densities and dissolved CO_2 levels, in a single wafer spin cleaning tool, MegPie®. Dissolution of increasing amounts of CO_2 in air saturated DI water caused a significant decrease in the number of breakages to line structures and also decreased the lengths of the line breakages, at all power densities up to 2.94 W/cm^2. This ability of dissolved CO_2 to protect against feature damage correlates well with its ability to suppress sonoluminescence in sound irradiated DI water.

Introduction

Megasonic cleaning is routinely employed in the semiconductor industry for removal of contaminant particles and residues from wafer surface. With the progression of technology nodes to smaller sizes, megasonic cleaning is faced with the challenge of maintaining high cleaning efficiency without inducing damage to small features (~100 nm and less). Judicious choice of cleaning chemicals and control of dissolved gases has been proposed to minimize wafer damage (1).

Sonoluminescence (SL), the phenomenon of release of light when liquid is irradiated by sound waves of sufficient intensity, is a sensitive indicator of cavitation events (2). It is widely believed that acoustic cavitation is responsible for both wafer cleaning and damage. Intensity of SL correlates with intensity of cavitation, mostly transient cavitation that is believed to cause damage to wafer features. Therefore, control of transient cavitation has potential application in controlling damage.

The authors of this paper have previously reported the strong ability of dissolved CO_2 to quench SL generation in DI water (3). It was shown that increasing amounts of dissolved CO_2 progressively decreased SL and ~150 ppm dissolved CO_2 was found to be sufficient to suppress SL generation in DI water under all conditions of power density and duty cycle of acoustic energy at frequency 0.93 MHz. It was also shown that CO_2 is not just incapable of supporting SL generation in DI water, but also a strong inhibitor of SL generation in the presence of other gases that support SL generation (3).

This paper reports the results from a systematic study conducted to measure the effect of dissolved CO_2 levels on wafer damage during megasonic exposure. Damage studies were conducted on two different line/space structures that were exposed to megasonic irradiation in a single wafer spin cleaning tool, MegPie®. Our results indicate a strong effect of dissolved CO_2 levels and acoustic power density on the extent of wafer damage during megasonic irradiation.

Materials and Methods

All experiments were conducted in class 100 micro/nano fabrication center at The University of Arizona. Study on damage caused by megasonic irradiation was conducted on two different model test structures; structures-I (provided by IMEC) and structures-II (provided by FSI international). The structures were subjected to megasonic irradiation in a single wafer spin cleaning tool, MegPie®.

MegPie® consists of a radial transducer array (area 32.3 cm^2), designed to apply uniform acoustic energy to a rotating substrate (0-60 rpm) at a frequency of 0.925 MHz, as shown in Fig. 1. Acoustic power density can be generated in the range 0.15 - 2.94 W/cm^2. MegPie® was configured for a distance of ~1.5 mm between the transducer and the wafer surface. However the distance between the test sample (affixed to the wafer) and the transducer was ~0.8 mm.

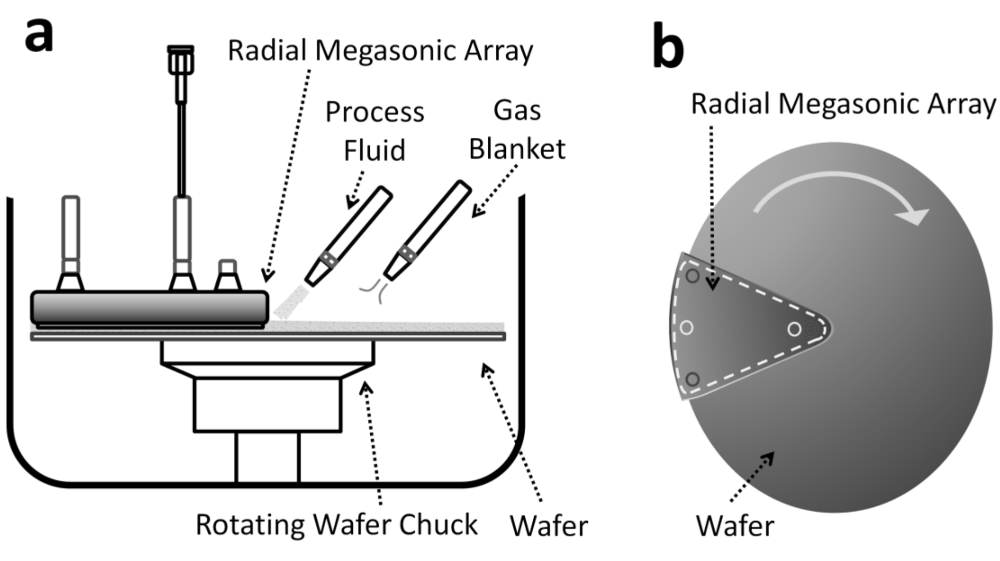

Figure 1. Schematic sketch of the single wafer spin-cleaning tool MegPie®. (a) Cross-sectional view and (b) top view.

Test structures-I (provided by Imec) were made from gate stacks consisting of HfO_2/AlO followed by nitridation anneal, 5 nm TiN, 5 nm Si and 100 nm a-Si. The patterned structure consisted of long (~2 mm) array of lines of width ~36 nm and separation ~523 nm, as shown in Fig. 2. Test structures-II (provided by FSI international) were made from Sematch 890AZ reticle. It consisted of array of long (~4 mm), thin (~67 nm) and thick (~113 nm) pairs of polysilicon lines on silicon substrate separated by a distance of ~630 nm. The pair of thick and thin lines were separated from each other by a distance of ~1300 nm (Fig. 2).

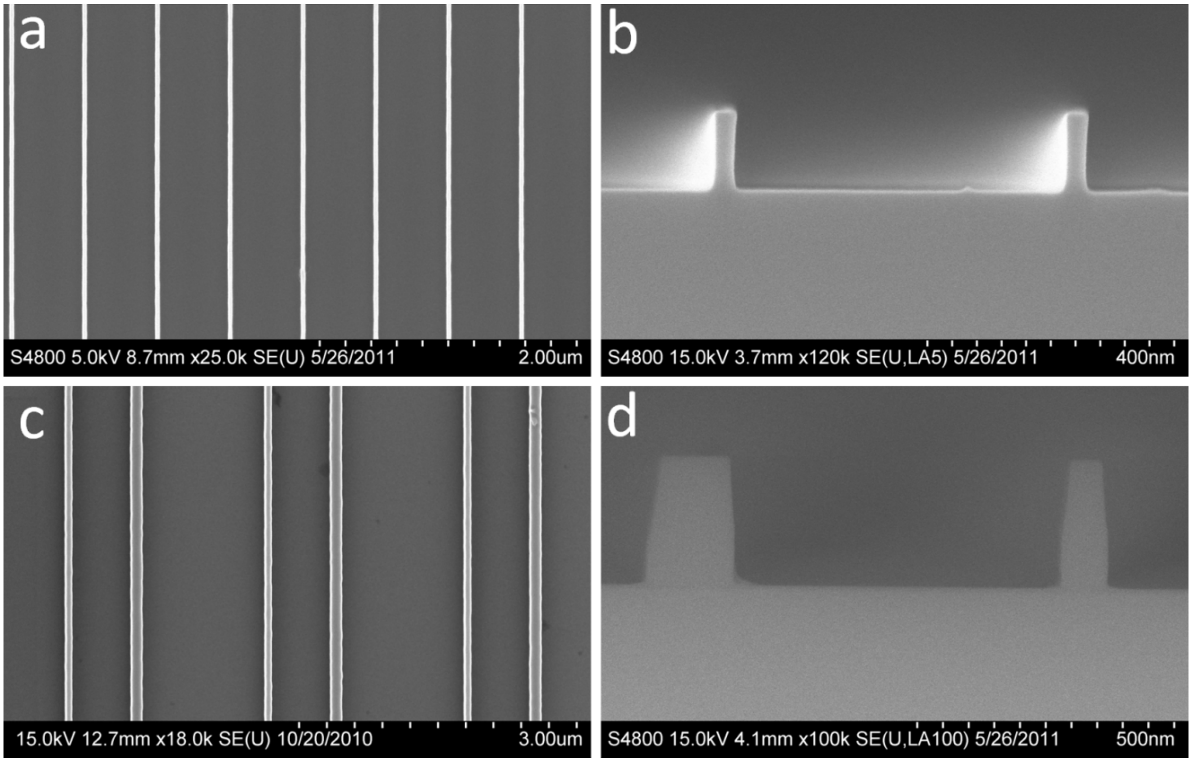

Figure 2. FESEM images of line structures-I and line structures-II. (a) Top view and (b) cross-sectional view of line structures-I. (c) Top view and (d) cross-sectional view of line structures-II.

Wafer samples of size 2 cm x 2 cm were excised from the test structures using a diamond scriber under DI water. They were then cleaned in APM (1:1:5) for 2 min, rinsed in DI water and then dried using IPA. Samples were quickly examined under optical microscope (Leica DM4000 M) at a magnification 200X, to ensure that the structures were clean and damage-free before megasonic irradiation. For each experiment, one sample was attached to an eight inch bare silicon wafer using a thin (~2 mm wide) double-stick adhesive tape placed away from the area bearing the line structures. A point at a radial distance of 2 inches from the centre of the wafer was marked and all samples were stuck at this point. DI water containing either dissolved air (saturation level) or different concentrations of dissolved CO_2 was dispensed on the surface of the substrate at a rate of 300 ml/min while the substrate was rotated at 30 rpm. The transducer array was then switched on to generate acoustic energy at a given power density for 2 min. Samples were then dried in open air for 5 min. To generate varying levels of dissolved CO_2 in DI water, CO_2 gas was bubbled in DI water and the resulting changes in pH were monitored using a pH meter. Dissolved CO_2 concentrations were calculated from the measured pH values using the following equation that results from the carbonic acid equilibria in water, established upon CO_2 dissolution (4).

$$[CO_2] \approx \frac{10^{7-2\times pH} - 10^{-7}}{4.25} \text{ M} \qquad [1]$$

A blanket of CO_2 on top of the spinning wafer was necessary to reach a high concentration of 1035 ppm of dissolved CO_2. Concentrations of CO_2 reported in this study were calculated based on the pH of the exit stream from the MegPie® during the 2 min period of exposure to megasonic irradiation.

Damages resulting from the exposure to megasonic energy were examined at low resolutions using an optical microscope and at high resolutions using a field emission scanning electron microscope (Hitachi S-4800, FESEM) (Fig. 3 and Fig. 4). For structures-I, width of the line features were small (~36 nm) and could not be resolved in an optical microscope. At a magnification of 200X, a large number of damage sites covering a representative area (0.3 mm x 0.4 mm) of the wafer, could be adequately resolved. These damage sites appeared as small dark spots (Fig. 3). Images for ten non-overlapping and contiguous regions of damages, covering an area of 1.2 mm^2 and occurring at a given power density, were collected and counted using the particle analysis tool in ImageJ (version 1.43u). For test structures-II, width of the lines were thick enough (~67 nm) to resolve in an optical microscope. A representative area of 0.08 mm^2 constituting ten pairs of thin and thick lines was examined and the damage sites were counted manually. Total number of damages (line breakages) for both structures were scaled to 1 mm^2 area of the wafer and plotted as a function of power density (Fig 5).

Results and Discussion

Fig. 3 shows optical microscope and FESEM images of line breakages occurring in test structures-I resulting from megasonic irradiation at a power density 2.5 W/cm^2. Fig. 3a and Fig. 3b are the optical microscope images of damages resulting in air saturated DI water and CO_2-saturated DI water (~1035 ppm CO_2), respectively. Comparison of Figs. 3a and 3b readily reveal the effectiveness of suppression of damage that is imparted by dissolved CO_2. Figs. 3c, 3d and 3e show FESEM images of damage resulting in DI water containing 0.5 (saturated with air), 412 and 1035 ppm of dissolved CO_2, respectively. As seen in these images, the number density of damages decreases with increasing dissolved CO_2 content in DI water. In addition, the size of line breakages occurring in air-saturated DI water (Fig. 3c) was seen to be larger than in CO_2 added DI water (Figs. 3d and 3e). The average size of line breakages occurring in air-saturated DI water and CO_2 added DI water was found to be ~1150 nm and ~770 nm, respectively. The average size of line breakages did not change significantly with change in power density. Fig. 3f presents a high magnification view of a typical line breakage occurring in either air-saturated or CO_2 added DI water. As seen in the figure, breakage occurs within the line-feature, forms a U-shape and leaves residual material sticking on the surface. These morphological features of line breakages remained largely unchanged with change in power density or nature of dissolved gas.

Fig. 4 shows FESEM images of line breakages occurring in structures-II in either air-saturated DI water (Fig. 4a) or CO_2-saturated DI water (Fig. 4b), at a power density 1.5 W/cm^2. As seen in these figures, damage occurred only to the thin lines close to the base of the line features, rather than inside the body of the line features; this is in contrast to the nature of damage observed with structures-I. As observed in case of structures-I, the number density of damage sites decreased upon addition of CO_2 and / or reduction of power density, but the morphological features of the damage sites remained largely unchanged.

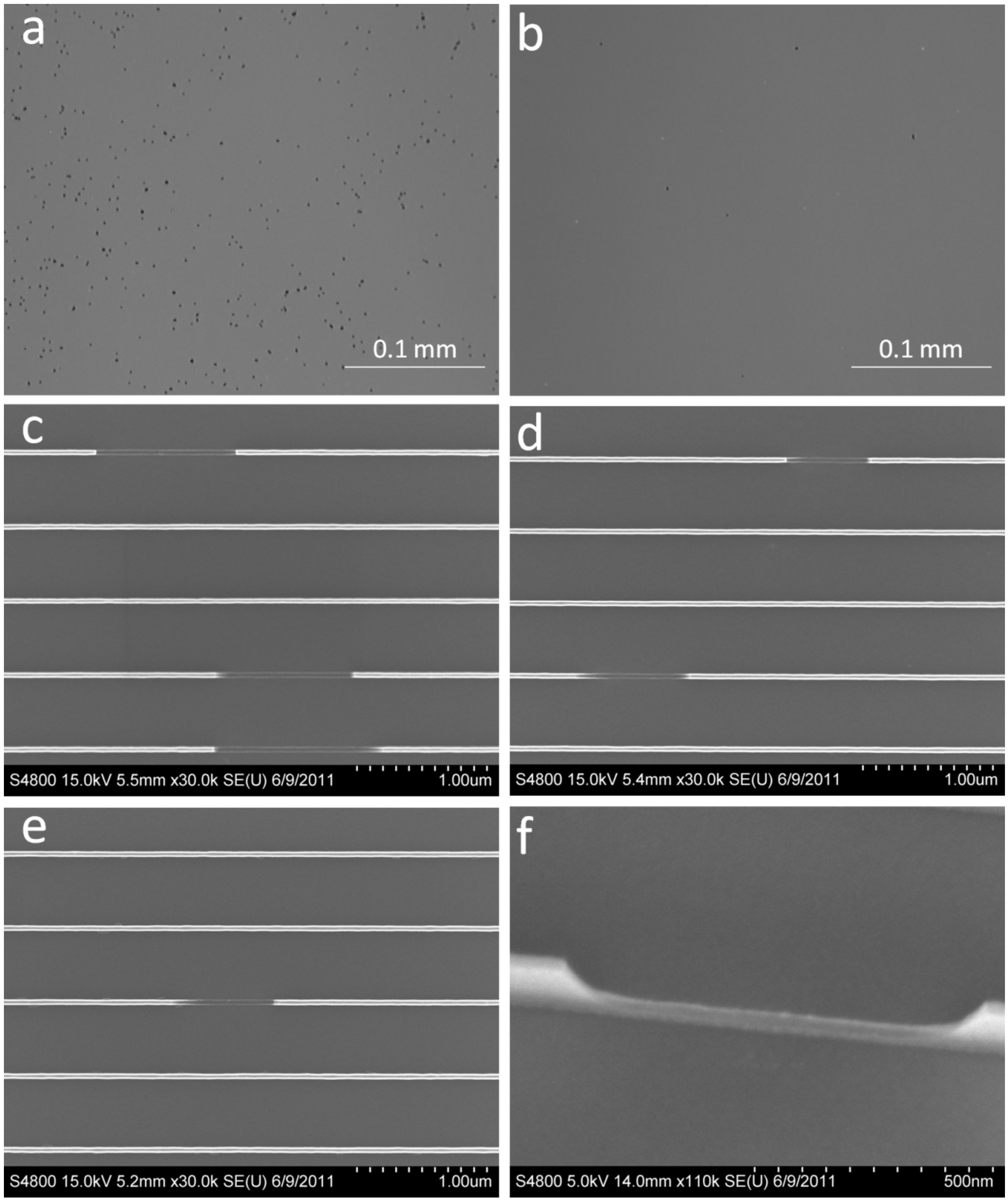

Figure 3. Microscope images of line breakages in Structures-I. (a,b) Optical microscope images at 200X and (c,d,e) FESEM images of line structures-I after 2 min irradiation to sound waves of power density 2.5 W/cm^2. (f) FESEM image of a typical damage site at high magnification. (a,c,f) Damage induced in air saturated DI water. Damage induced in (c) 0.5 ppm CO_2-DI water, (d) 412 ppm CO_2-DI water and (e) 1035 ppm CO_2-DI water.

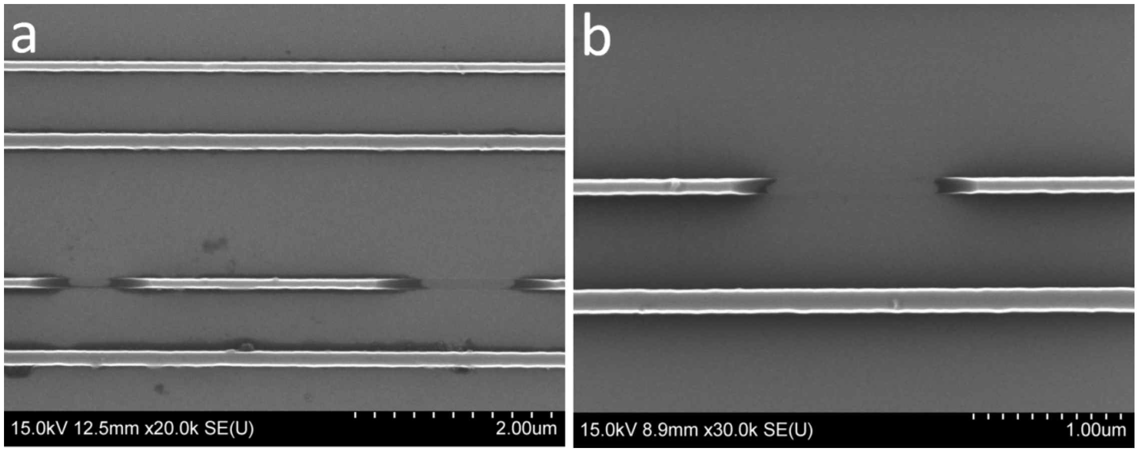

Figure 4. FESEM images of line breakages in Structures-II. FESEM images of line structures-II after 2 min irradiation to sound waves of power density 1.5 W/cm^2 in (a) air saturated DI water and (b) 1035 ppm CO_2-DI water.

Fig. 5 shows a plot of the number of line breakages as a function of power density and level of dissolved CO_2 occurring in structures-1 (Fig. 5a) and structures-II (Fig. 5b). In case of both structures, a strong suppression of damage was observed upon addition of CO_2 to DI water. The extent of suppression of damage increases in a dose-dependent manner with the increase in concentration of dissolved CO_2, as seen in Fig 5a.

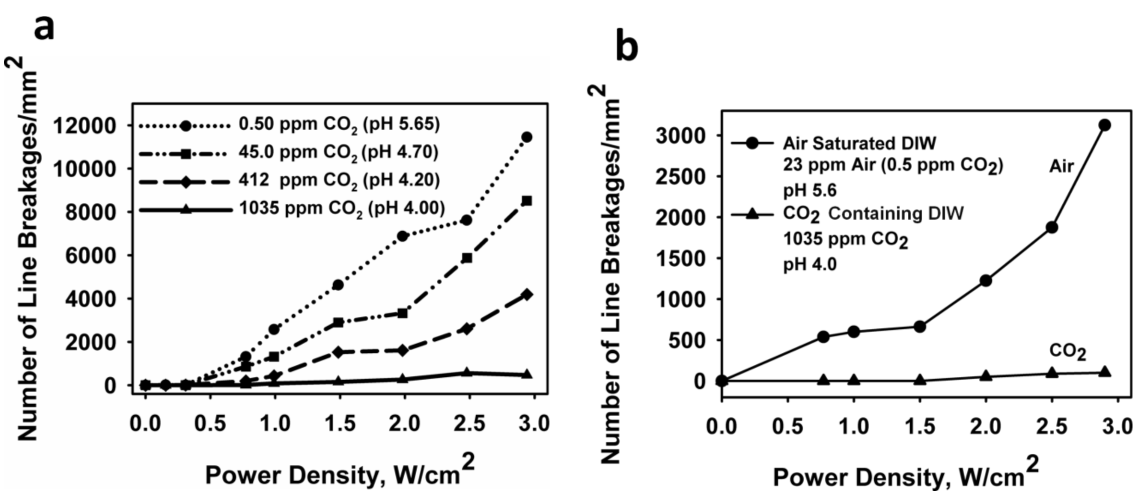

Figure 5. Plot of number density of line breakages in structures-I and structures-II as a function of megasonic power density and dissolved CO_2 levels in DI water. (a) Structures-I and (b) structures-II.

This study demonstrates that a strong correlation exists between the suppression of SL and suppression of damage caused by dissolved CO_2. It was previously shown that dissolution of increasing amounts of CO_2 progressively decreases SL generation in DI water. Taken together, these results support the hypothesis that dissolved CO_2 reduces wafer damage through suppression of damage causing violent cavitation events, known as transient cavitation. It may be noted that CO_2 gas has much higher solubility (~ 1500 ppm) in water compared to air (~ 23 ppm). Therefore, higher amounts of CO_2 gas can diffuse into the cavity during the expansion phase and may cushion the subsequent collapse. However, our results do not rule out the possibility that CO_2 may also suppress stable cavitation that is thought to be primarily responsible for damage-free cleaning. Cleaning studies on the effect of dissolved CO_2 on contaminant removal efficiency in sound irradiated DI water would be necessary to further understand the mechanism of protection imparted by dissolved CO_2. In addition to cavitation, pH is also an important parameter affecting particle removal from wafer surfaces. Since CO_2 dissolution decreases pH, measurements of the effect of dissolved CO_2 levels on cavitation-assisted particle removal would require that pH be maintained constant at varying levels of dissolved CO_2. Methods to generate varying CO_2 levels, while holding pH at a constant value of choice, have been demonstrated by us, previously (5).

Conclusions

The number density of line breakages increases with acoustic power density and decreases with increasing levels of dissolved CO_2 content in DI water. The average size of line breakages also decreases upon addition of CO_2 in DI water. The nature of breakage was found to depend on the material composition of the line features but not the nature of dissolved gas. Megasonic irradiation of DI water caused damage to line features of thicknesses 67 and 35 nm, but not to lines of thickness 113 nm. In structures-II, numerous damages were observed on the thin line (~67 nm) but no damages were seen on the thick line (~113 nm) at any power density studied, suggesting that these line structures become highly susceptible to megasonic damage below a critical thickness. Taken together, these results confirm a strong effect of dissolved CO_2 in suppressing damage to wafers during their megasonic processing under varying conditions of power density and material composition of wafer features.

Acknowledgments

Authors affiliated with the University of Arizona gratefully acknowledge the financial support and loan of the single wafer spin tool by ProSys Inc and the donation of test structures by IMEC and FSI international.

References

1. G. Vereecke, F. Holsteyns, S. Arnauts, S. Beckx, P. Jaenen, K. Kenis, M. Lismont, M. Lux, R. Vos, J. Snow and P. W. Mertens, in *Ultra clean processing of silicon surfaces vii*, P. Mertens, M. Meuris and M. Heyns Editors, p. 141 (2005).
2. A. J. Walton and G. T. Reynolds, *Adv. Phys*., **33**, 595 (1984).
3. S. Kumari, M. Keswani, S. Singh, M. Beck, E. Leibscher, P. Deymier and S. Raghavan, *Microelectron Eng*., (2010). doi:10.1016/j.mee.2010.10.036
4. S. Kumari, M. Keswani, M. Beck, E. Leibscher, T. Liang, P. Deymier and S. Raghavan, *ECS Transactions,* **25**, 5, 295–302 (2010).
5. S. Kumari, M. Keswani, S. Singh, M. Beck, E. Leibscher, P. Deymier and S. Raghavan, *Control of Sonoluminescence in Deionized Water Exposed to Megasonic Field*. UCPSS, Belgium, 20-22 Sep 2010.